Research Article
Vol. 24, No. 26 | 26 Dec 2016 | OPTICS EXPRESS 30309
Optics EXPRESS

# Nonlinear compensation with DBP aided by a memory polynomial

João Gonçalves,[1,3] Celestino S. Martins,[1,4] Fernando P. Guiomar,[2] Telmo R. Cunha,[1] José C. Pedro,[1] Armando N. Pinto,[1] and Pedro M. Lavrador[1]

[1] *Department of Electronics, Telecommunications and Informatics, University of Aveiro and Instituto de Telecomunicações, 3810-193, Aveiro, Portugal*
[2] *Dipartimento di Elettronica e Telecomunicazioni, Politecnico di Torino, Corso Duca degli Abruzzi, 24, 10129 Torino, Italy*
[3] *jpfg@ua.pt*
[4] *csmartins@av.it.pt*

**Abstract:** Using digital backpropagation (DBP) based on the split step Fourier method (SSFM) aided by a memory polynomial (MP) model, we demonstrate an improved DBP approach for fiber nonlinearity compensation. The proposed technique (DBP-SSFM&MP) is numerically validated and its performance and complexity are compared against the benchmark DBP-SSFM, considering a single-channel 336 Gb/s PM-64QAM transmission system. We demonstrate that the proposed technique allows to maintain the performance achieved by DBP-SSFM, while decreasing the required number of iterations, by over 60%. For a transmission length of 1600 km we obtain a complexity reduction gain of 50.7% in terms of real multiplications in comparison with the standard DBP-SSFM.



**OCIS codes:** (060.2330) Fiber optics communications; (060.1660) Coherent communications.

## References and links

1. R.-J. Essiambre, G. Kramer, P. J. Winzer, G. J. Foschini, and B. Goebel, "Capacity limits of optical fiber networks," J. Lightw. Technol. **28**(4), 662–701 (2010).
2. A. Carena, V. Curri, G. Bosco, P. Poggiolini, and F. Forghieri, "Modeling of the impact of nonlinear propagation effects in uncompensated optical coherent transmission links," J. Lightw. Technol. **30**(10), 1524–1539 (2012).
3. E. Ip and J. M. Kahn, "Compensation of dispersion and nonlinear impairments using digital backpropagation," IEEE/OSA J. Lightw. Technol. **26**(10), 3416–3425 (2008).
4. S. J. Savory, G. Gavioli, E. Torrengo, and P. Poggiolini, "Impact of interchannel nonlinearities on a split-step intrachannel nonlinear equalizer," IEEE Photon. Technol. Lett. **22**, 673–675 (2010).
5. D. S. Millar, S. Makovejs, C. Behrens, S. Hellerbrand, R. I. Killey, P. Bayvel, and S. J. Savory, "Mitigation of fiber nonlinearity using a digital coherent receiver," IEEE J. Sel. Topics Quantum Electron. **16**(5) 1217–1226, (2010).
6. F. Yaman and G. Li, "Nonlinear impairment compensation for polarization-division multiplexed WDM transmission using digital backward propagation," IEEE Photonics Journal, (2), 816–832 (2010).
7. F. P. Guiomar and A. N. Pinto, "Simplified Volterra series nonlinear equalizer for polarization-multiplexed coherent optical systems," J. Lightw. Technol. **31**(23), 3879–3891 (2013).
8. E. Giacoumidis, I. Aldaya, M. Jarajreh, A. Tsokanos, S. T. Le, F. Farjady, Y. Jaouen, A. Ellis, and N. Doran, "Volterra-based reconfigurable nonlinear equalizer for coherent OFDM," IEEE Photon. Technol. Lett. **26**(14), 1383–1386 (2014).
9. G. Shulkind and M. Nazarathy, "Nonlinear digital back propagation compensator for coherent optical OFDM based on factorizing the Volterra series transfer function," Opt. Express **21**(11), 13145–13161 (2013).
10. V. Parahyba, J. Reis, S. Ranzini, E. Schneider, E. Rosa, F. Simões, J. Diniz, L. Carvalho, E. Filho, J. Oliveira, and J. Oliveira, "Performance against implementation of digital backpropagation for high-speed coherent optical systems," Electron. Lett. **51**(14), 1094–1096 (2015).
11. D. Rafique, M. Mussolin, M. Forzati, J. Mårtensson, M. N. Chugtai, and A. D. Ellis, "Compensation of intra-channel nonlinear fibre impairments using simplified digital back-propagation algorithm," Opt. Express **19**(10), 9453–9460 (2011).
12. M. Secondini, S. Rommel, G. Meloni, F. Fresi, E. Forestieri, and L. Potì, "Single-step digital backpropagation for nonlinearity mitigation," Photonic Network Communications **31**(3), 493–502 (2016).
13. F. P. Guiomar, S. B. Amado, C. S. Martins, and A. N. Pinto, "Time domain Volterra-based digital backpropagation for coherent optical systems," J. Lightw. Technol. **15**(33), 3170–3181 (2015).

#280876
http://dx.doi.org/10.1364/OE.24.030309
Journal © 2016
Received 14 Nov 2016; revised 13 Dec 2016; accepted 14 Dec 2016; published 22 Dec 2016

Optics EXPRESS

14. S. B. Amado, F. P. Guiomar, N. J. Muga, R. M. Ferreira, J. D. Reis, S. M. Rossi, A. Chiuchiarelli, J. R. F. Oliveira, A. L. Teixeira, and A. N. Pinto, "Low complexity advanced DBP algorithms for ultra-long-haul 400G transmission systems," J. Lightw. Technol. **34**(8), 1793–1799 (2016).
15. A. Napoli, Z. Maalej, V. Sleiffer, M. Kuschnerov, D. Rafique, E. Timmers, B. Spinnler, T. Rahman, L. Coelho, and N. Hanik, "Reduced complexity digital back-propagation methods for optical communication systems," J. Lightw. Technol. **32**(7), 1351–1362 (2014).
16. J. Kim and K. Konstantinou, "Digital predistortion of wideband signals based on power amplifier model with memory," Electron. Lett. **37**, 1417–1418 (2001).
17. D. R. Morgan, Z. Ma, J. Kim, M. G. Zierdt, and J. Pastalan, "A generalized memory polynomial model for digital predistortion of RF power amplifiers," IEEE Trans. Signal Process **54**, 3852–3860 (2006).
18. L. C. Vieira and N. J. Gomes, "Experimental demonstration of digital predistortion for orthogonal frequency-division multiplexing-radio over fibre links near laser resonance", IET Optoelectronics **9**(6), 310-316 (2015).
19. A. Tehrani and H. Cao, "A comparative analysis of the complexity/accuracy tradeoff in power amplifier behavioral models," IEEE Trans. Microw. Theory Tech. **58**, 1510–1520, (2010).
20. S. J. Savory, "Digital filters for coherent optical receivers," Opt. Express **16**(2), 804–817 (2008).
21. Y. J. Liu, W. Chen, J. Zhou, B. H. Zhou, and F. M. Ghannouchi, "Digital Predistortion for Concurrent Dual-Band Transmitters Using 2-D Modified Memory Polynomials," IEEE Trans. Microw. Theory Tech, **61** (1), 281-290 (2013).

## 1. Introduction

The capacity bottleneck in the current optical transmission systems is primarily dictated by the Kerr effect and its interaction with chromatic dispersion (CD) along the fiber link [1,2]. In order to perform fiber nonlinearity compensation, several techniques based on the digital backpropagation (DBP) concept have been proposed, namely through split-step Fourier methods (SSFM) [3–6] and Volterra series nonlinear equalizers (VSNE) [7–9]. Despite the high effectiveness of DBP-based techniques to compensate the fiber nonlinearity, their main drawback comes from the high complexity requirements, due to the large number of iterations, for a practical implementation [10]. This limitation has motivated several investigations towards reduced complexity algorithms [11–15]. Nevertheless, there is still a need for solutions that enable their practical application.

DSP-based algorithms for fiber nonlinearity mitigation have been widely proposed using the DBP-SSFM technique, enabling the trade-off between performance and complexity as a function of number of iterations. In this regard, weighted SSFM (W-SSFM) has been proposed as a promising approach, enabling a significant reduction of the number of iterations when compared with the standard SSFM [11]. Enhanced SSFM (ESSFM) has been also proposed in [12], allowing the decrease of computational effort and latency over SSFM, while keeping the same performance. Alternatively, DBP techniques based on VSNE have been also proposed as an attempt to further reduce the complexity associated to the DBP-based implementations [7, 13]. In this respect, weighted VSNE (W-VSNE), has been proposed in [13] and its experimental assessment has been provided in [14], revealing further improvement in terms of the computational effort and latency, over the standard SSFM and W-SSFM. Despite these significant improvements, there are several models developed in wireless communication, which can be explored in optical systems to increase the transmission linearity, while minimizing the equalizer complexity. Among these models, the memory polynomial (MP) algorithm has revealed to be an attractive solution, enabling to provide a good trade-off between performance and complexity [16, 17]. Previous approaches [18] have considered the use of the MP model as predistorter in Radio over Fiber links with good performance results. In this work they have adopted a post compensation strategy to circumvent the problem of the backlink required for the predistorter estimation. In addition, a detailed analysis of the complexity implementation of MP, in terms of number of floating point operations, has been also provided in [19].

We propose an alternative approach for fiber nonlinearity compensation with DBP, by combining the MP technique and the standard SSFM. Then, for validating the method, we conduct a comparative analysis, in terms of performance and complexity of the proposed technique against the standard SSFM. For a long-haul single-channel PM-64QAM optical link, we demonstrate a reduction of 50% in terms on real multiplications (RMs).

The remaining of this paper is organized as follows: in Section 2, a theoretical background for the SSFM and MP is provided; the computational effort behind the two approaches is presented in Section 3; in Section 4, the numerical results for the performance and complexity are presented; finally, the conclusions drawn from this work are summarized in Section 5.

## 2. DBP-based SSFM aided by memory polynomial

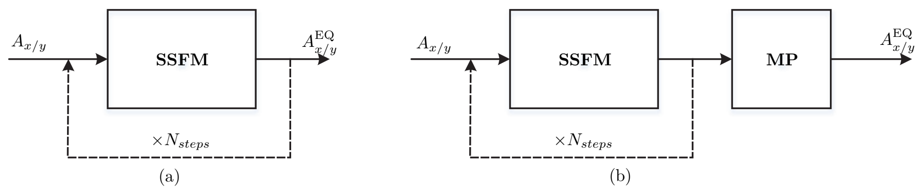


Fig. 1. Simplified implementation diagram of (a) DBP-SSFM and (b) DBP-SSFM aided by MP.

The basic idea behind DBP concepts is that the received signal is backward propagated through virtual fibers, with the inverse characteristics of the transmission fiber. In the case of polarization-multiplexed optical signal, the backward propagation in a single-mode fiber can be analytically described by the inverse Manakov equation [6] as,

$$\frac{\partial A_{x/y}}{\partial(-z)} = \frac{\alpha}{2}A_{x/y} + i\frac{\beta_2}{2}\frac{\partial^2 A_{x/y}}{\partial t^2} - i\frac{8\gamma}{9}\left(|A_x|^2 + \left|A_y\right|^2\right)A_{x/y}, \tag{1}$$

where $A_{x/y}$ is the slowly varying complex field envelope in the $x/y$ states of polarization, and $z$ and $t$ are the spatial and temporal coordinates, respectively. The fiber parameters $\alpha$, $\beta_2$ and $\gamma$ are defined as the attenuation coefficient, dispersion parameter and nonlinear coefficient, respectively. The practical implementation of DBP has been widely performed through the SSFM, which is an iterative method, where the virtual link is divided into smaller segments over which the field solution is estimated. For each segment, the chromatic dispersion and nonlinearity are decoupled from the nonlinear Schrödinger equation and compensated separately. Usual implementation of SSFM in DBP is performed using an asymmetric algorithm, where the linear step is performed followed by the nonlinear step, as

$$A^{\mathrm{EQ}}_{x/y}(t_n, z) = A^{\mathrm{CD}}_{x/y}(t_n, z)\exp\left[-i\frac{8}{9}\xi\gamma h_{eff}\left(|A^{\mathrm{CD}}_x(t_n, z)|^2 + |A^{\mathrm{CD}}_y(t_n, z)|^2\right)\right], \tag{2}$$

where $A^{\mathrm{EQ}}_{x/y}$ and $A^{\mathrm{CD}}_{x/y}$ corresponds to the equalized signal and the linear equalized signal component in the $x/y$ polarization, respectively, at the discrete time instant, $t_n$. The optimization parameter, $\xi$, is defined in the range $0 < \xi \leq 1$ and $h_{eff}$ represents the effective step-size given as,

$$h_{eff} = \frac{\exp(\alpha h) - 1}{\alpha} \tag{3}$$

where $h$ defines the spatial step-size. The CD equalization is usually performed in frequency-domain (FD), using fast Fourier transform (FFT)/inverse fast Fourier transform (IFFT) algorithms to switch between FD and time domain (TD) representation of the signal. In addition, the employment of overlap-save/add method is required to allow the implementation in continuous time. The equalized samples are then provided as the input to the next fiber segment, which is repeated for the entire fiber link. The correspondent implementation diagram is shown in Fig. 1(a).

Though the SSF method has revealed high accuracy, which improves with increasing number of iterations, its extensive complexity is prohibitive for any real-time application. Therefore, it is critical to reduce the complexity of numerical methods in DBP. In this context, we introduce the MP model after DBP-SSFM to relax the overall implementation complexity requirements, while guaranteeing the same performance. Based on this idea we can achieve the DBP-SSFM&MP model illustrated in Fig. 1(b). This approach enables to further improve the performance of DBP-SSFM in the scenario where the ideal DBP-SSFM is limited by some practical constrains, such as the electrical and optical noise. It should be noted that the ideal DBP-SSFM could be achieved in absence of electrical and optical noise. In this sense, it allows to reduce the number of iterations, $N_{steps}$, employed in DBP-SSFM by utilizing larger step-size, $h$, while maintaining the same performance of DBP-SSFM. Therefore, the key requirement is that the complexity incurred by the MP stage is low enough so that the overall complexity of DBP-SSFM&MP becomes lower than DBP-SSFM. Note that the parameter $N_{steps}$ interferes heavily on the total complexity of DBP-based techniques.

MP has been extensively used in wireless communication as an effective method to reduce the complexity requirements associated to the general implementation of Volterra series, and at the same time providing a good performance [17]. Basically, the MP model is a truncation of the general Volterra model in which only diagonal terms of the Volterra kernels are considered and is commonly formulated as,

$$y(n) = \sum_{k=1}^{K} \sum_{m=0}^{M} c_{k,m} x(n-m) |x(n-m)|^{k-1}, \tag{4}$$

where $x(n-m)$ and $y(n)$ are the complex baseband input and output signals, respectively and $c_{k,m}$ are the polynomial coefficients. $K$ is the nonlinearity order and $M$ is the memory depth, which accounts the effect of $\frac{M}{2}$ past samples and future $\frac{M}{2}$ samples. In this work MP is applied to each polarization independently, and according to the Fig. 1(b), $x(n-m)$ corresponds to the output of SSFM in $x/y$ states of polarization and $y(n)$ corresponds to the equalized sample after MP in $x/y$ states of polarization. An important advantage of this model is that the coefficients appear in linear form, which, besides facilitating their estimation through the least-squares-type algorithms, imposes that the complexity of MP evolves linearly with $K$ and $M$ [19].

## 3. Computational effort

In this section, we analyze the computational effort associated with DBP-SSFM and DBP-SSFM&MP, based on the number of RMs per equalized sample. We have assumed the implementation of linear equalization in the FD using the overlap-save method. Therefore, considering the FFT block-size of $N_{FFT}$ and the memory length of CD over the fiber-optic channel of $N_M$, a number of $N_{FFT} - N_M + 1$ samples per FFT can be compensated. $N_M$ can be estimated following [20], while $N_{FFT}$ is set larger than $N_M$ and can be optimized to minimize the number of operations per equalized sample.

### *3.1. Split-step Fourier method*

The computational effort associated with SSFM can be divided into linear and nonlinear components. For each polarization, the linear component requires the computation of 1 FFT and 1 IFFT for the signal switching between TD/FD and $N_{FFT}$ complex multipliers (CMs) for the multiplication of signal spectra with CD transfer function. Considering the two polarizations and the Cooley-Tukey FFT algorithm, the total number of CMs can be given as [15],

$$N_{CD} = 8N_{FFT} \left(\log_2(N_{FFT}) + 1\right). \tag{5}$$

The nonlinear component requires the computation of $2N_{FFT}$ squared moduli operations, $N_{FFT}$ RMs for nonlinear phase rotation and $2N_{FFT}$ CMs to account for the multiplications between the input samples and the complex exponential outputs over the two polarizations. In this case, we have neglected the complexity of the complex exponential, since it can be implemented through look-up-tables (LUTs). Therefore, the total number of RMs for nonlinear component can be estimated as,

$$N_{NL} = 13N_{\text{FFT}}. \tag{6}$$

The overall number of RMs per equalized sample for $N_{steps}$ SSFM can be estimated as,

$$N_{SSFM} = \frac{N_{steps}\,(N_{CD} + N_{NL})}{N_{FFT} - N_M + 1}. \tag{7}$$

### 3.2. Memory polynomial model

Following the study presented in [19], we have performed the evaluation of the computational effort associated with the MP technique considering two implementation stages for the expression (4): the construction of basis functions, $x(n-m)|x(n-m)|^{k-1}$; and the filtering of basis with the kernels, $c_{k,m}$. In the construction of the basis function it is only required to generate the term $x(n)|x(n)|^{k-1}$ since all other $x(n-m)|x(n-m)|^{k-1}$ can be obtained by delaying the existing terms. Assuming that the square root of moduli of $x(n)$ is implemented through LUTs, the required number of RMs to construct the basis function is estimated as,

$$N_{basis} = 2K, \tag{8}$$

and the required number of RMs with respect to the filtering stage is estimated as,

$$N_{filter} = 4K(M+1). \tag{9}$$

Therefore, the complexity of one MP can be obtained by the summation of these two components, $N_{MP} = N_{basis} + N_{filter}$, and the overall complexity of DBP-SSFM&MP is achieved by including the complexity associated with DBP-SSFM and the factor of 2 over $N_{MP}$ to account the complexity of the two polarizations. The complexity of DBP-SSFM&MP can be given as,

$$N_{SSFM\&MP} = N_{SSFM} + 2N_{MP}. \tag{10}$$

## 4. Numerical simulation

In order to validate the proposed DBP-SSFM&MP approach, we have performed the simulation of a single-channel 336 Gb/s PM-64QAM transmission system using VPItransmissionMaker. The generated PM-64QAM signal is sent to the recirculating loop considering different number of spans of 80 km of standard single-mode fiber (SSMF), which is characterized by $\alpha = 0.2$ dB/km, $\beta_2$ of -20.4 ps/nm/km and $\gamma$ of 1.3 $\text{W}^{-1}\text{km}^{-1}$. Losses are recovered at the end of each fiber span by an Erbium-doped fiber amplifier (EDFA) with 5-dB noise figure. The received electrical fields are then fully post-processed in MATLAB, including the following main DSP subsystems: The static equalization, with respect to the static fiber impairments, such as chromatic dispersion and nonlinear distortion, is performed by DBP-SSFM and DBP-SSFM&MP equalizers, for different number of steps, $N_{steps}$. In the case of DBP-SSFM&MP equalizer, before the application of MP, we have performed the signal interpolation to 4 samples per symbol, which is then aligned with the transmitted signal. A frame of 30000 symbols of these signals are used to perform the estimation of MP coefficients, $c_{k,m}$, using a least mean square algorithm; Linear adaptive equalization is then performed by means of constant modulus algorithm (CMA). The resulting signal is downsampled to 1 sample per symbol after which a phase recovery is applied. Finally, the symbol decoding is performed and the bit-error-rate (BER) is evaluated over $2^{19}$ received bits.

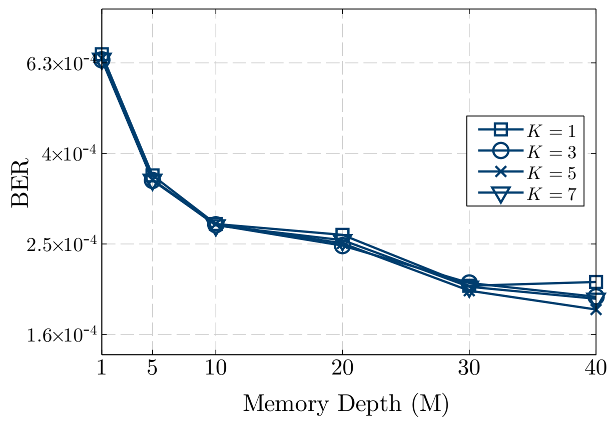


Fig. 2. Evaluation of BER as a function of memory deep, $M$, considering different nonlinearity order, $K$. The transmission length is 800 km. The results have been obtained using DBP-SSFM&MP with 8 steps and 4 dBm input power.

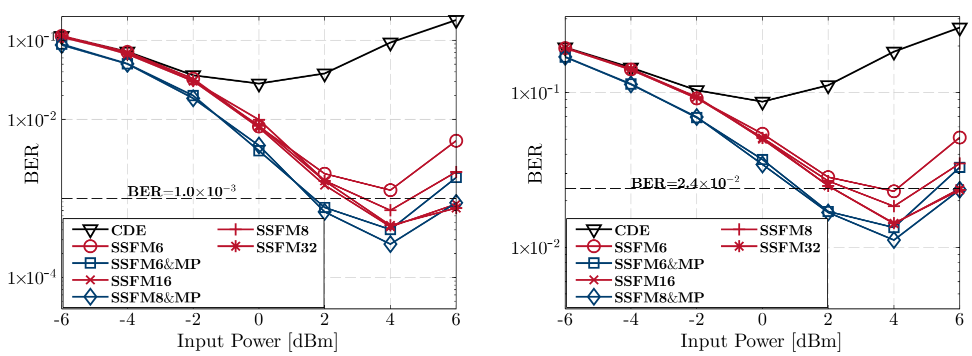


(a) (b)

Fig. 3. BER as function of input power for DBP-SSFM and DBP-SSFM&MP; (a) transmission length of 800 km and (b) transmission length of 1600 km.

### *4.1. Performance assessment*

In order to identify the best model for DBP-SSFM&MP, which improves the trade-off between the performance and complexity in comparison with the standard DBP-SSFM, we have performed the numerical simulations considering different algorithm parameters, such as the number of iterations, $N_{steps}$, the nonlinearity order, $K$, and the memory depth, $M$. In both cases, the linear equalization is performed in FD, using FFT/IFFT algorithms in conjunction with overlap-save method. For each considered transmission length, the FFT block-size applied in linear equalization, $N_{FFT}$, is defined such that penalty-free CD equalization is ensured with the minimum complexity. Therefore, we have estimated $N_{\text{FFT}}$ as the next power of two of $6N_M$, where $N_M$ is the number of taps determined according to [20]. Taking into account these considerations, we have initiated our analysis with the evaluation of BER as a function of $M$ for different values of $K$, and considering the transmission length of 800 km, as depicted in Fig. 2. We can note that the performance of DBP-SSFM&MP improves with increasing $M$ and $K$, and tends to saturate for $M > 30$. This, indicates that a window of 30 neighboring samples is enough to characterize the phase shifts induced by CD. Regarding the parameter $K$, we can note a slight

Optics EXPRESS

increase of performance with increasing $K$, and this inspection evidences a low impact of higher order terms of the Volterra model in DBP-SSFM&MP. Taking into account a trade-off between the performance and complexity, we have identified the MP model parameters as, $K = 1$ and $M = 10$ for the subsequent analysis. In this case, the MP assistance is kept linear, performing as a linear equalizer after DBP-SSFM. Nevertheless, the MP provides the post-compensation system some redundancy in case the nonlinear parameter of the fiber used in DBP-SSFM is not exact and some nonlinearity residue appears uncompensated.

After evaluating the impact of parameters $M$ and $K$ on the performance of DBP-SSFM&MP, we have proceeded to the evaluation of BER as a function of input power for DBP-SSFM and DBP-SSFM&MP, considering different number of iterations, $N_{steps}$. In addition, we have also presented the results when only linear equalization is performed. In order to obtain a more comprehensive comparison, we have considered two scenarios for the transmission length of 800 km and 1600 km, with a defined BER limit of $1\times10^{-3}$ and $2.4\times10^{-2}$, respectively. The obtained results for these two scenarios are presented in Figs. 3(a) and (b), respectively. First of all, it is evident that the nonlinearity compensation achieves higher performance than the CD compensation only, which remains well above defined BER threshold in both scenarios. Besides, in both scenarios the minimum BER for nonlinearity compensation is achieved at launch power of 4 dBm, whereas for the linear compensation it is obtained at launch power of 0 dBm. By comparing the two approaches for nonlinearity equalization, we can note that DBP-SSFM&MP outperforms DBP-SSFM both in the linear and nonlinear operating regime and that the performance of DBP-SSFM saturates at 16 steps. This saturation is due to the presence of electrical and optical noise, which limits the achievement of ideal DBP-SSFM. From the Fig. 3(a), it can be noted that the minimum BER achieved for DBP-SSFM using 6 steps (DBP-SSFM6) is still above the defined BER threshold, whereas the minimum BER achieved by DBP-SSFM&MP using 6 steps (DBP-SSFM6&MP) is far bellow the defined BER threshold and is similar to the maximum performance attained by DBP-SSFM16. This improvement can be explained by the inclusion of MP method, which takes into account the correlation between neighboring samples to compensate the residual phase shifts still left by DBP-SSFM and by the fact that the MP is evaluated using more samples per symbols then the DBP method, allowing a better noise filtering. According to this analysis, we can note that a significant reduction on the number of iterations can be achieved by employing DBP-SSFM&MP instead of DBP-SSFM, in this case obtaining a reduction over 60%. Similar conclusions can be also taken from Fig. 3(b). In addition to this analysis, Fig. 3 also illustrates further flexibility, in terms of trade-off between performance and complexity, of DBP-SSFM&MP over DBP-SSFM. In this regard, we can observe that DBP-SSFM8&MP beyond outperforming DBP-SSFM16, enables a reduction of the value of $N_{steps}$ to 50%. As it is shown in the following, this reduction can have a considerable impact on the overall algorithm complexity.

Although the proposed method is validated in single-carrier scenario, it can in principle be applied in a scenario using superchannels and can in principle be extended to a multi-channel scenario by using multiple input memory polynomial models [21]. Nevertheless, this is something that need to be further investigated.

Table 1. Computational effort of the DBP-SSFM versus DBP-SSFM&MP for $N_{FFT} = 256$, $K = 1$ and $M = 10$.

| | DBP-SSFM16 | DBP-SSFM6&MP | DBP-SSFM8&MP |
|---|---|---|---|
| $N_{\mathrm{RMs}}$ | 1554.3 | 766.9 | 961.1 |
| $G_{\mathrm{R}}$ (%) | – | 50.7 | 38.2 |

Optics EXPRESS

### 4.2. Computational effort comparison

We assess the complexity of DBP-SSFM&MP and DBP-SSFM, as a function of parameter $N_{steps}$, considering the case of study presented in Fig. 3 and following the expressions presented in Section 3. It can be noticed some degree of flexibility for DBP-SSFM&MP over DBP-SSFM, which allows to optimize the value of $N_{steps}$ for a given targeted BER. In order to explore this flexibility we have performed the comparison of a given $N_{steps}$ for DBP-SSFM against different values of $N_{steps}$ for DBP-SSFM&MP. As a figure of merit we have adopted the reduction gain, $G_{\mathrm{R}}$, in percentage, defined as $G_R = (1 - O/O_{\mathrm{ref}})$, where $O$ and $O_{\mathrm{ref}}$ are the number of operations required by DBP-SSFM&MP and DBP-SSFM, respectively. In order to take into account the oversampling factor of 2, due to the signal interpolation to 4 samples per symbol before the employment of MP, we have multiplied the value of $N_{MP}$ by 2. In this regard, Table 1 presents the complexity of DBP-SSFM&MP in comparison with DBP-SSFM in terms of RMs. We can observe that DBP-SSFM6&MP achieves a reduction gain over 50% over DBP-SSFM16, while their performances are the same. This result illustrates that although MP imposes an additional complexity over DBP-SSFM, it enables a significant reduction of $N_{steps}$, which allows an overall complexity reduction. On the other hand, we can note that DBP-SSFM8&MP provides a reduction gain of 38.2%, and at the same time higher performance than DBP-SSFM16. These results clearly evidence that DBP-SSFM&MP imposes a better trade-off between performance and complexity than the standard DBP-SSFM.

## 5. Conclusion

By cascading a nonlinear MP model equalizer and DBP-SSFM, we have proposed a new approach for nonlinearity compensation in optical transmission systems. Considering a single-channel 336 Gb/s PM-64QAM transmission system, we have demonstrated that DBP-SSFM&MP outperforms the conventional DBP-SSFM, enabling a significant reduction in the number of iterations for similar performance. The comparison of complexity between the two approaches reveals an extensive gain reduction for DBP-SSFM&MP with respect to DBP-SSFM, over 50%. The obtained results indicate that the combination of MP with DBP is a promising approach to reduce the complexity associated with DBP-based techniques.

## Funding

FCT/MEC through national funds and when applicable co-funded by FEDER PT2020 partnership agreement under the project UID/EEA/50008/2013 (actions VADONet-C and SoftTransceiver), and Ph.D. grant PD/BD/113817/2015.